Chemical Engineering Journal 175 (2011) 291–297

Contents lists available at SciVerse ScienceDirect

Chemical Engineering Journal

journal homepage: www.elsevier.com/locate/cej

# Monoamine-grafted MCM-48: An efficient material for $CO_2$ removal at low partial pressures

Marta Gil[a], Inés Tiscornia[b], Óscar de la Iglesia[a,c], Reyes Mallada[a,d,*], Jesús Santamaría[a,d,**]

[a] Institute of Nanoscience of Aragón (INA) and Chemical and Environmental Engineering Department, Universidad de Zaragoza, Zaragoza, Spain
[b] Instituto de Investigaciones en Catálisis y Petroquímica, INCAPE (FIQ, UNL-CONICET), Santiago del Estero 2829, 3000 Santa Fe, Argentina
[c] Institute of Nanoscience of Aragón (INA), Centro Universitario de la Defensa, Ctra. de Huesca s/n, E-50090 Zaragoza, Spain
[d] Ciber de Bioingeniería, Biomateriales y Nanomedicina (CIBER-BBN), Edificio I+D, Mariano Esquillor S/N, 50018 Zaragoza, Spain

ARTICLE INFO

*Article history:*
Received 27 July 2011
Received in revised form
23 September 2011
Accepted 23 September 2011

*Keywords:*
MCM-48
Mesoporous silica
Functionalization
APTES
$CO_2$ adsorption

ABSTRACT

Mesoporous cubic MCM-48 material was synthesized and functionalized with 3-aminopropyltriethoxysilane (APTES) under different conditions and used for $CO_2$ adsorption. Before and after functionalization the materials were characterized by different techniques: XRD, TEM, TGA, fluorescence analysis of amino and adsorption–desorption isotherms of $N_2$ and $CO_2$. The results confirmed that $CO_2$ adsorption in amino modified materials involves both chemisorption and physisorption. The former is the primary mechanism at low partial pressures, and includes the formation of carbamates. This material demonstrated a high efficiency for $CO_2$ removal at low $CO_2$ partial pressures, with loadings of 0.5 mmol$CO_2$/molN at 5 kPa. The maximum adsorption capacity at 1 atm of $CO_2$ was 1.68 mmol/g.



## 1. Introduction

Although $CO_2$ removal from gas streams is routinely carried out in different industrial applications, the efforts aimed to the capture and storage of $CO_2$ to mitigate climate change in recent years have eclipsed traditional applications. Traditionally, separation of $CO_2$ has been carried out by absorption with chemical reaction using aqueous solutions of alkanolamines, mainly monoethanolamine (MEA), diethanolamine (DEA) and methyldiethanolamine (MDEA). However, energy consumption associated with the use of liquid amines is high because of solvent regeneration, and large dilutions with water are required to prevent equipment corrosion and flow problems caused by amines. For many applications, regenerable solid adsorbents are considered as an advantageous alternative over liquid absorption since they are more environmentally benign and easier to handle, and most importantly, they have lower energetic requirements for regeneration.

A recent review of Choi et al. describes extensively the materials used for $CO_2$ adsorption [1], discussing important aspects such as kinetics, regenerability and stability, in addition to adsorption capacity. These materials include conventional porous adsorbents such as zeolites or activated carbons, and chemisorbents such as calcium and magnesium oxides, lithium zirconates, hydrotalcites, and organic–inorganic hybrid materials. Drawing inspiration from the liquid amine $CO_2$ scrubbing process, surface modification with amine groups has been used to enhance $CO_2$ adsorption on porous solids including more traditional materials such as zeolites and activated carbon, and novel solids such as carbon nanotubes [2,3], metal–organic frameworks (MOFs) capable of a high adsorption capacity at high $CO_2$ pressures [4,5], and a variety of mesoporous silicas (MS) with which this work is concerned. The wide pore sizes that can be engineered in MS (ca. 2–20 nm), and their active surface containing numerous silanol groups available for reaction have made them popular for amino functionalization, as described in recent reviews [1,6].

The interaction of $CO_2$ with amine groups in a water-free environment gives rise to carbamates, via the formation of the $CO_2$-amine zwitterion, such as $RNH_2{}^+COO$ [7]. Overall this reaction requires two amine groups per $CO_2$ molecule, i.e. an adsorption efficiency, defined as the $CO_2$/N molar ratio, equal to 0.5.

$$RNH_2 + CO_2 \rightarrow RNH_2{}^+COO^-$$

$$RNH_2{}^+COO^- + RNH_2 \rightarrow RNHCOO^- + RNH_3{}^+$$

It is important to notice that in the amine surface for the formation of bidentate carbamate neighbour amines are needed, which

* Corresponding author. Tel.: +34 976 761000x5440.
** Corresponding author. Tel.: +34 976 761153.
*E-mail addresses:* rmallada@unizar.es (R. Mallada), Jesus.Santamaria@unizar.es (J. Santamaría).

1385-8947/$ – see front matter © 2011 Elsevier B.V. All rights reserved.
doi:10.1016/j.cej.2011.09.107

means that a homogeneous coverage should be achieved in the surface of the material. On the other hand, when water is present, a molar $CO_2$/N ratio of 1 can be achieved due to the contribution of bicarbonate and carbonate species. The formation of the carbamate involves an equilibrium and it is, therefore, reversible: complete regeneration of the adsorbent has been previously confirmed by other authors [7,8]. It is also important to point out that, while this mechanism corresponds to chemisorption physisorption also takes place at higher partial pressures. In order to evaluate only chemisorption a low pressure of $CO_2$, such as 5 kPa, should be considered [9,10].

To increase the adsorption capacity of amino-functionalized mesoporous silica the preferred method consists of increasing the amount of amino groups in the grafted material. However, in view of the adsorption mechanism presented for mono, di and tri-amines [7], the highest efficiency, defined as the mole of adsorbed $CO_2$/mol N, would be encountered in monoamine for $CO_2$ adsorption under humid conditions.

Focusing on monoamine-functionalized mesoporous silica materials the review of the available data gives efficiency values ranging from 0.09 to 0.89 [1,6]. This suggests that the functionalization process either has a low reproducibility or, more likely, varies strongly for materials with different structures and pore sizes. In fact the highest values (around 0.5 in dry conditions, and at low partial pressures of carbon dioxide, where mainly chemisorption takes place) are encountered for the pore-expanded MCM-41, PE-MCM-41 developed by Harlick and Sayari [6], and the three-dimensional pore structure MCM-48 [8]. The 3-D structure is important because their interconnected pores are expected to facilitate access first to the functionalization agents that produce amino groups on the silica, and then to the $CO_2$ molecules to be captured. To our knowledge, only three publications [8,11,12] investigate $CO_2$ adsorption on amino-functionalized MCM-48, and the reported adsorption capacity, at 1 atm $CO_2$ pressure varies from 0.8 to 2.05 mmol/g.

In this work we have functionalized the 3-D MCM-48 siliceous structure, using 3-aminopropyltriethoxy-silane under different conditions, then we have characterized the resulting structures and their behaviour in $CO_2$ adsorption, with the aim of relating the adsorption performance to material properties such as the amount of amino groups anchored to the surface, surface area, pore volume and crystallinity.

## 2. Experimental

### 2.1. Synthesis of MCM-48

MCM-48 was prepared by liquid-phase hydrothermal synthesis from a gel with the following molar composition: 1.4 $SiO_2$: 1.0 CTABr: 0.35 $Na_2O$: 5.0 EtOH: 140 $H_2O$ [13]. A silicate solution was used as the silica source, hexadecyltrimethylammonium bromide (CTABr) as the structure-directing agent, and ethanol as additive for the mesophase control. The precursor reactants used were Ludox AS40 (40% $SiO_2$: 60% $H_2O$, Sigma–Aldrich), sodium hydroxide (98 wt%, Panreac), CTABr (Sigma–Aldrich), ethanol absolute (Panreac) and deionized water.

To prepare the silica source, Ludox was slowly incorporated to an aqueous solution of NaOH 1 M with vigorous stirring. The molar composition of the resultant mixture was 0.25 $Na_2O$: 1.0 $SiO_2$: 12.5 $H_2O$. This mixture was heated to 343 K for 1 h, then the solution was cooled to room temperature. In a separate vessel, the surfactant, cetyl trimethyl ammonium bromide (CTABr), was dissolved in an EtOH/$H_2O$ mixture with a molar composition of 1 CTABr: 5.0 EtOH: 120 $H_2O$.

The silica source was added to the surfactant solution at room temperature, and the mixture was stirred for 1 h. The amount of gel prepared in a batch was 70 g and it was poured either in two Teflon-lined stainless steel autoclave, ($V$ = 43 mL) or in a glass laboratory flask ($V$ = 250 mL) and subjected to a hydrothermal treatment for 4 days at 373 K. The solid product was filtered, washed with hot water and dried overnight. Finally, calcination at 813 K in air was carried out to eliminate the surfactant.

### 2.2. Functionalization with amines

For the functionalization with 3-aminopropyltriethoxy-silane (APTES, Sigma–Aldrich), 125 mg of MCM-48 powder were dispersed in 7.5 mL of dry toluene in a flask under stirring in an inert atmosphere. Then, a volume between 0.04 and 0.26 mL of APTES was added. The mixture was stirred at reflux temperature, 383 K, for time varying from 1 to 5 h. The treated mesoporous material was vacuum filtered, washed with $CH_2Cl_2$/ether (1:1) and dried at 323 K for 24 h.

### 2.3. Amino-groups titration

This determination of the amount of amino groups is based in reaction of the non-fluorescent fluorescamine with the primary amines, which yields a fluorescent derivative [14]. The fluorescence spectrum was measured by excitation at 396 nm in Fluorescence Spectrometer (PerkinElmer LS 55), and emission intensity at 486 nm was measured. Calibration solutions were prepared following the procedure developed by Ritter and Brühwiler [15]. To carry out the reaction with fluorescamine, a 100 μL aliquot of this solution was transferred to a cuvette and 2 mL of phosphate buffer (0.2 M, pH 8.0) and 1 mL of fluorescamine solution (1 mM in acetone) were added. For the analysis, the same procedure was followed but adding 15 mg of amino-functionalized MCM-48 to an aqueous solution of NaOH 0.02 M instead of the APTES solution.

The amount of APTES on functionalized MCM-48 powders was also analysed by means of thermogravimetric analyses (TGA), using a TA Instruments Q5000 analyzer, with a heating rate of 5 °C/min up to 1173 K under air atmosphere. The weight loss between 403 K and 1073 K was attributed to the loss of the organic groups and the amount of N was calculated using the equivalence of 71 mg of weight loss per mmol of N, (which corresponds to the APTS molecule grafted to two silanol groups). This leads to a reliable estimation of the amount of amino groups, as can be seen from the comparison between the TGA method and the fluorescamine method given in Table 4. Further weight loss up to 1173 K was negligible (around 0.01%).

In some samples the N content was analysed using an elemental analysis technique with a PerkinElmer 2400 analyzer. A good correlation was observed among the results obtained by the three methods (fluorescamine titration, TGA and elemental analysis) and therefore the determination of amino groups was in general done by TGA, which allowed a faster and more convenient analysis.

### 2.4. Characterization

Nitrogen adsorption isotherms were measured at 77 K on Micromeritics ASAP 2020 and Micromeritics TriStar 3000 analyzers. $CO_2$ adsorption isotherms were obtained in the same equipment at 298 K, fixed amounts of $CO_2$ were dosed to the sample and the equilibrium pressure achieved was measured starting from low pressure around 0.03 atm up to 1 atm. Degassing conditions of non-functionalized MCM-48 powder were 8 h at 473 K under vacuum. For the functionalized MCM-48 samples, degassing was carried out for 10 h at 383 K under vacuum. The BET specific surface area was calculated using the BET equation in the linear range. Pore volume was calculated at a relative pressure of 0.95.

**Table 1**
Synthesis batches for MCM-48.

| Sample | Synthesis yield (%) | BET area ($m^2/g$) | Pore volume ($m^3/g$) |
|---|---|---|---|
| P1 | 45.1 | 1364 | 1.047 |
| P4 | 46.8 | 1225 | 1.017 |
| P6A | 46.6 | 1394 | 0.979 |
| P6B | | 1378 | 0.996 |
| P2 | 43.4 | 1333 | 1.132 |
| P7 | 53.8 | 1471 | 1.134 |
| P8 | 51.5 | 1427 | 0.994 |
| P11 | 54.5 | 1376 | 1.044 |
| P12 | 54.3 | 1371 | 1.019 |
| P13 | 56.0 | 1155 | 0.951 |
| | 50.2 ± 4.7 | 1349 ± 93 | 1.031 ± 0.06 |
| P9 | 61.0 | 1000 | 0.600 |
| P10 | 44.0 | 1130 | 0.736 |
| P14 | 58.0 | 1184 | 0.811 |

X-ray diffraction analyses were carried out using a Philips X'Pert MPD diffractometer with Cu Kα radiation. The diffraction data were recorded in the 2θ range of 0.6–8° with a scanning rate of 5 s/step (step 2θ = 0.02). TEM images were obtained using a FEI TECNAI T20 at 200 kV.

## 3. Results and discussion

### 3.1. Synthesis of MCM-48: reproducibility and characterization

In view of the already noted discrepancies in the literature, if was deemed essential to ensure that the characteristics of the starting MCM-48 material were highly homogeneous, since this material was going to be functionalized under different conditions and then used for $CO_2$ adsorption. Thirteen different batches of 70 g of synthesis gel were prepared, subjected to hydrothermal synthesis, calcined and characterized by nitrogen adsorption, as seen in Table 1. Ten out of the thirteen samples show almost identical isotherm, type IV. The mean values of these ten samples for BET specific surface area and pore volume were 1349 ± 93 $m^2/g$ and 1.031 ± 0.061 $cm^3/g$, these samples were mixed to give the starting MCM-48 material source. The other three samples possessed a significantly lower pore volume, between 0.6 and 0.81 $cm^3/g$ and were discarded for the functionalization study.

Fig. 1 shows the XRD diffraction pattern of some of the synthesised samples and the diffraction angles correspond to the ones previously reported for MCM-48 [16]. It could be observed that the main diffraction angle [2 1 1] at 2.26 shifts to higher values, 2.5 after calcination which is attributed to shrinkage of the structure during the removal of the surfactant.

### 3.2. Study of the functionalization conditions

#### 3.2.1. Influence of the concentration of APTES

The functionalization of the mesoporous material implies the reaction between the silanol groups in the surface and the ethoxyl groups of the silane. Regarding this point, an estimation of the amount of free hydroxyl groups in the surface is necessary to guarantee that the amount of silane suffices for functionalization. Several estimations for hydroxyl groups in siliceous material can be found in the literature, Zhuravlev [17], estimate 4.9 Si–OH/$nm^2$ in amorphous silica, for SBA-15 the value is 2.2 Si–OH–/$nm^2$ [10], and 1.8 Si–OH–/$nm^2$ in the case of MCM-41 and MCM-48 [18]. The amount of silanol groups also depends on the treatment of the sample, and the temperatures it is subjected to, as shown by Knowles et al. [19], who prepared hexagonal mesoporous silica HMS with two different contents of silanol groups depending upon the conditions for surfactant removal: calcination led to 2 Si–OH–/$nm^2$ while ethanolic extraction yielded 5 Si–OH–/$nm^2$.

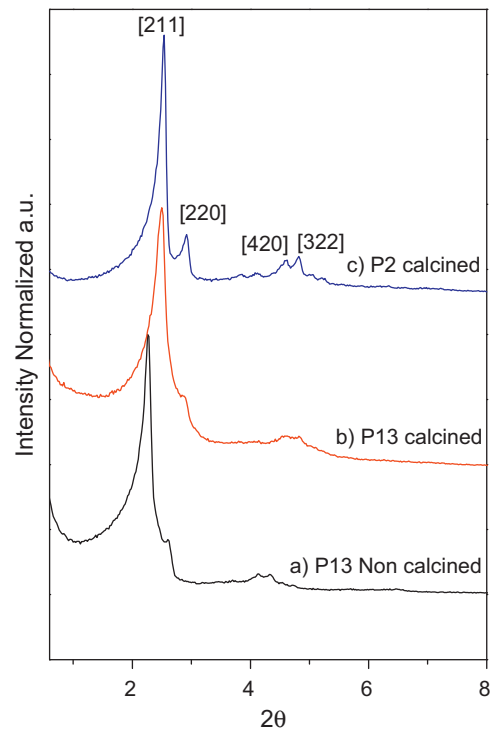


**Fig. 1.** Diffraction patterns of (a) sample P13 before calcination, (b) sample P13 after calcination, (c) sample P2 after calcination.

Since our samples were calcined at 813 K, a value of 2 Si–OH/$nm^2$ seems reasonable for the samples in this work. Considering that each APTES molecule reacts with a surface silanol group and that only 50% of the OH groups in the surface can be modified due to steric hindrance [20], for a BET surface area of 1349 $m^2/g$, the "stoichiometric" amount would correspond to 1.04 mL APTES/g MCM-48.

Three functionalization experiments were carried out with concentrations of APTES corresponding to 2.08, 1.04 and 0.32 mL/g of MCM-48, respectively, with a reaction time of 2 h. $N_2$ and $CO_2$ adsorption/desorption isotherms of these samples are presented in Fig. 2, together with that for an unfunctionalized MCM-48 sample. Table 2 gives the structural and $CO_2$ adsorption characteristics for the same materials. Reversibility of the adsorption process was studied with one sample subjected to four cycles of adsorption/desorption, not shown, the standard deviation of the maximum $CO_2$ adsorption capacity was 2.3%. It can be seen that, as the amount of APTES used for functionalization increases, the BET surface area and pore volume decrease rapidly (from 1155 to 422 $m^2/g$ and from 0.95 to 0.25 $cm^3/g$ respectively. In spite of this decrease, increasing the concentration of APTES (and therefore the degree of functionalization) causes a 120% enhancement of $CO_2$ adsorption, from 0.52 to 1.14 mmol/g. This enhancement is caused by the chemisorption that takes place between $CO_2$ and the $NH_2$ present in APTES, while only physisorption takes place in the non-functionalized sample.

#### 3.2.2. Influence of reaction conditions

Experiments were carried out at a fixed concentration of APTES ($2.08 \times 10^{-3}$ mL/mg) and increasing reaction times (1, 2 and 5 h). Table 3 summarizes the properties of these samples. In this case, the total amount of amino groups on the MCM-48 based on the elemental analysis is similar in all the samples and varies from 2.1 to 2.3 mmol N/g in good agreement with the maximum value reported in literature for this material [8]; however, the total amount of $CO_2$ adsorbed varies considerably, from 1.12 to 1.68 mmol/g. In

**Table 2**
Influence of the concentration of APTES used in the functionalization step. Reaction time: 2 h.

| | APTES concentration (mL/mg MCM-48) | BET surface area ($m^2/g$) | Pore volume ($cm^3/g$) | $CO_2$ adsorbed @ 101 kPa (mmol/g) | $CO_2$ adsorbed @ 5 kPa (mmol/g) | mmol N/g[a] | $\frac{mmol\ CO_2}{mmol\ N}$ [b] |
|---|---|---|---|---|---|---|---|
| P13 | – | 1155 | 0.95 | 0.52 | 0.04 | 0 | – |
| F1 | $2.08 \times 10^{-3}$ | 422 | 0.25 | 1.14 | 0.46 | 2.1 | 0.22 |
| F2 | $1.04 \times 10^{-3}$ | 751 | 0.34 | 1.02 | 0.24 | 1.4 | 0.17 |
| F3 | $0.32 \times 10^{-3}$ | 804 | 0.39 | 0.68 | 0.08 | 1.3 | 0.06 |

[a] Quantified by elemental analysis.
[b] Efficiency reported at 5 kPa partial pressure of $CO_2$.

**Table 3**
Influence of the reaction time used in the functionalization step. APTES concentration $2.08 \times 10^{-3}$ mL/mg.

| | Reaction time (h) | BET surface area ($m^2/g$) | Pore volume ($cm^3/g$) | $CO_2$ adsorbed @ 101 kPa (mmol/g) | $CO_2$ adsorbed @ 5 kPa (mmol/g) | mmol N/g | $\frac{mmol\ CO_2}{mmol\ N}$ [c] |
|---|---|---|---|---|---|---|---|
| F5 | 5 | 202 | 0.13 | 1.12 | 0.69 | 2.30[a] | 0.30 |
| F1 | 2 | 422 | 0.25 | 1.14 | 0.46 | 2.10[a] | 0.22 |
| F4 | 1 | 591 | 0.31 | 1.39 | 0.57 | 2.20[a] | 0.26 |
| F6 | 1 | 365 | 0.21 | 1.68 | 1.09 | 2.28[b] | 0.48 |
| F7 | 1 | 445 | 0.25 | 1.62 | 1.02 | 2.12[b] | 0.48 |
| F8 | 1 | 319 | 0.24 | 1.30 | 0.37 | 2.05[b] | 0.18 |

[a] Values from elemental analysis results.
[b] Values from fluorescamine method determination of amine groups.
[c] Efficiency reported at 5 kPa partial pressure of $CO_2$.

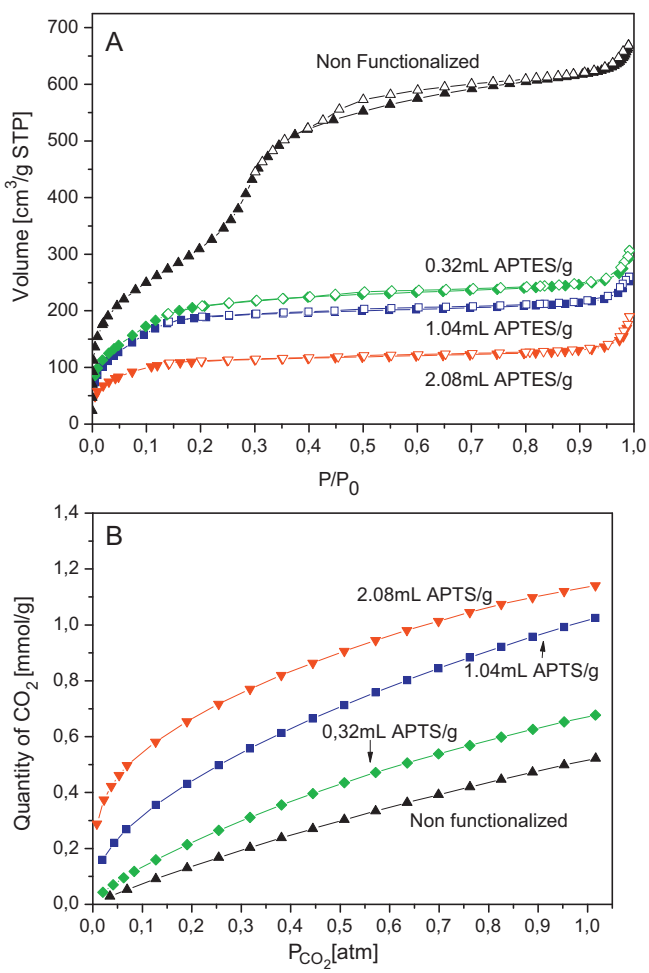


**Fig. 2.** $N_2$ (A) and $CO_2$ (B) adsorption–desorption isotherms for MCM-48 powder after calcination and for functionalized samples. Concentration of APTES: F1, 2.08 mL APTES/g; F2, 1.04 mL APTES/g; F3, 0.32 mL APTES/g MCM-48. Reaction time: 2 h. Stirring speed: 400 rpm.

particular, increasing the reaction time to 5 h lead to a dramatic drop in the pore volume and in the BET surface area. The XRD results of Fig. 3 indicate that there is already a clear decrease of crystallinity and order for the sample functionalized for 2 h, which is enhanced after 5 h of reaction time, leading to considerable structural damage. Clearly, the reaction conditions required for functionalization have a severe effect on the structural integrity of the MCM-48, which makes it necessary to limit the reaction time. The loss of crystallinity is observable even in one of the samples that had been subjected to shorter (1 h) reaction times. Thus, the XRD diagram corresponding to sample F8 in Fig. 3 presents a clear loss of

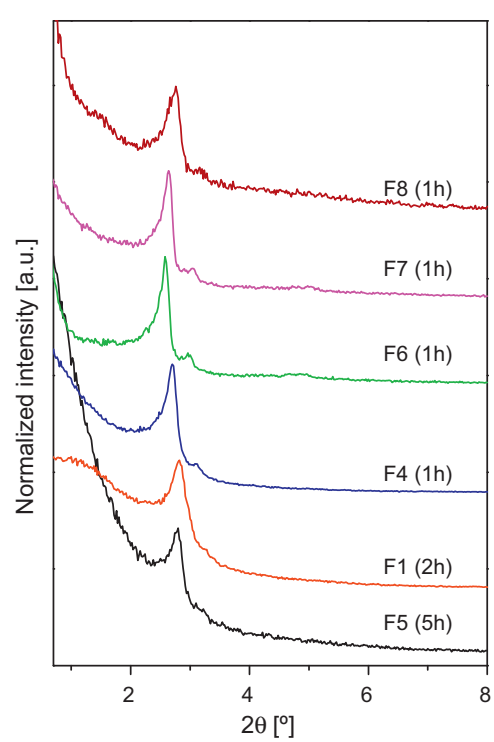


**Fig. 3.** Diffraction patterns of F5, F1, F4, F6, F7 and F8 samples, with different time of functionalization.

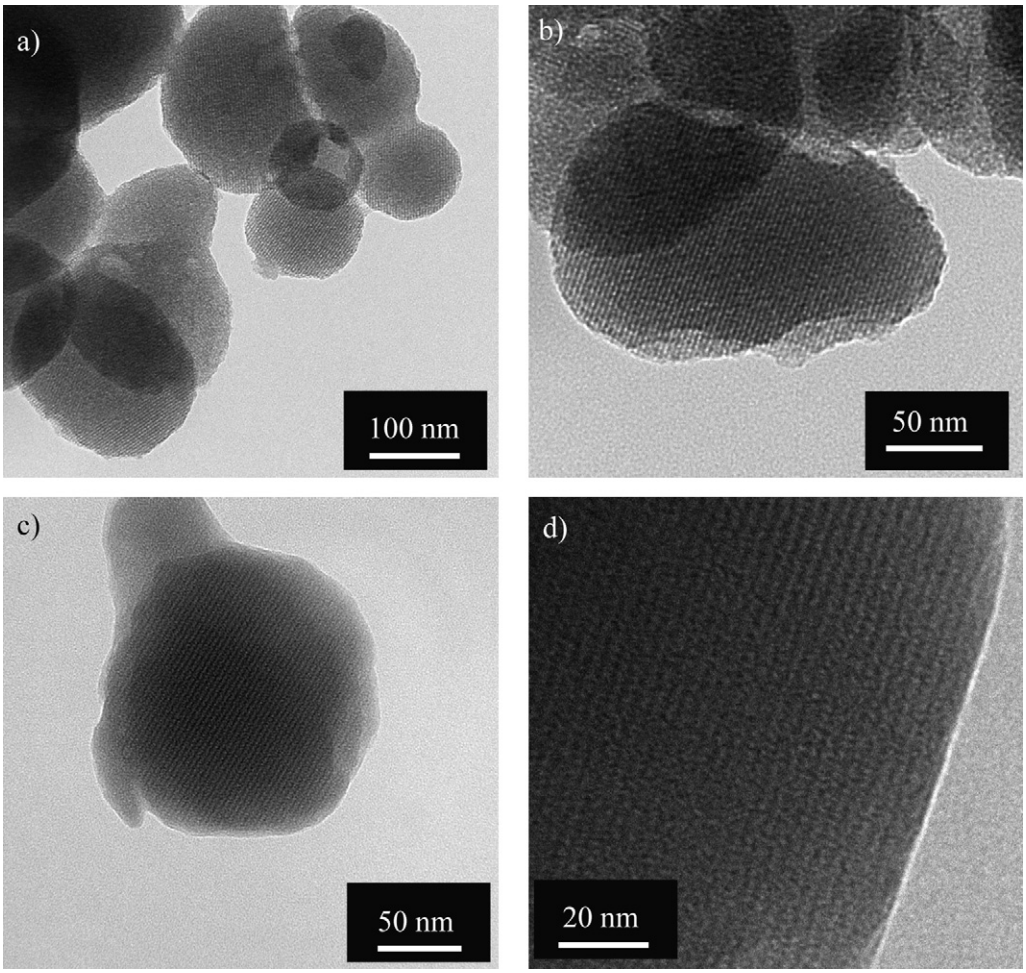


**Fig. 4.** TEM images of (a) and (b) MCM-48 powder after calcination; (c) and (d) sample F7, functionalized with APTES.

crystallinity when compared to that of samples F6 and F7, probably due to some slight variation in the reaction conditions.

It is interesting to note that, with some scatter, the values obtained for the chemisorption efficiency (last column of Table 3) are in a relatively narrow interval (0.18–0.48), with the sample subjected to a 5 h functionalization in an intermediate position regarding $CO_2$ efficiency (0.30). However this sample gave the lowest capacity for $CO_2$ adsorption (1.12 mmol/g), followed by the sample functionalized for 2 h (1.14 mmol/g), while all the samples functionalized for 1 h gave considerably higher values (1.30–1.68 mmol/g). This would suggest that the contribution of chemisorption to $CO_2$ capture is comparable for all the samples (as could be expected, given the similar concentration of amino groups), and the decrease of the total amount of adsorbed $CO_2$ in the samples functionalized for longer times would mainly be attributed to the loss of surface area and pore volume, as a result of the structural damage under reaction conditions, leading to a reduction of the physisorbed $CO_2$.

We can therefore conclude that long reaction times damage the structure and as result there is a loss in adsorption capacity. Regarding the samples functionalized for one hour, the lowest efficiency (0.18) corresponds to sample F8 that also presents the lowest crystallinity in the diffraction pattern (see Fig. 3) of all the samples functionalized for 1 h, suggesting that the structure also plays an important role in the chemisorption process. In contrast, the highest efficiency is observed for samples F6 and F7 where the structure after functionalization is largely intact. This can be inferred from the diffraction patterns of Fig. 3, and can be directly appraised in the TEM pictures of Fig. 4: well defined planes are present for sample F7, with a structural organization comparable to that of the non fuctionalized sample.

It is known that mesoporous silicas can collapse when they are mechanically compressed [21]. In order to minimize mechanical damage a set of samples was functionalized under a lower stirring speed, (200 rpm) during 1 h, using the highest concentration of APTES (2.08 mL/g). The characteristics of the samples are presented in Table 4. A lower functionalization degree was achieved, 1.71 mmol N/g as an average, measured by the fluorescamine method. As shown in Table 4, a very similar value is obtained from thermogravimetric analysis assuming that an average of two siloxane groups were anchored to the surface. The diffraction patterns of these samples (not shown) confirm that the structure was preserved, with the two main diffraction peaks corresponding to [2 1 1] and [2 2 0] clearly marked, indicating that structural damage had been minimized. However, the degree of surface functionalization is lower (1.7 vs. 2.2 mmol N/g), due to the slower reaction rate caused by the decreased mass transfer coefficients at a lower stirring speed. Accordingly, the $CO_2$ adsorption capacity is strongly diminished (maximum values around 1 mmol/g, compared to 1.68 mmol/g for sample F6 prepared at 400 rpm), even though the surface area of the samples prepared at 200 rpm is considerably larger (approximately 1000 $m^2$/g, compared to less than 400 $m^2$/g for sample F6).

**Table 4**
Samples with stirring speed 200 rpm.

| Sample | mg MCM-48 | BET surface area ($m^2/g$) | Pore volume ($cm^3/g$) | Maximum $CO_2$ adsorbed (mmol/g) | mmol N/g[a] | mmol N/g[b] | $\frac{mmol\ CO_2}{mmol\ N}$ [c] |
|---|---|---|---|---|---|---|---|
| F9 | 125 | 948 | 0.454 | 0.97 | 1.77 | 1.76 | 0.14 |
| F10 | 125 | 1094 | 0.498 | 0.95 | 1.74 | 1.64 | 0.16 |
| F11 | 125 | 1058 | 0.481 | 0.82 | 1.71 | 1.59 | 0.14 |
| F12 | 250 | 971 | 0.488 | 0.89 | 1.94 | 2.01 | 0.11 |
| F13 | 250 | 1034 | 0.462 | 0.95 | 1.69 | 1.74 | 0.16 |
| F14 | 250 | 1034 | 0.514 | 0.97 | 1.79 | 1.81 | 0.12 |
| F15 | 250 | 983 | 0.475 | 1.02 | 1.69 | 1.58 | 0.15 |

[a] Values from fluorescamine method.
[b] Values from thermogravimetric analysis.
[c] Efficiency reported at 5 kPa partial pressure of $CO_2$.

**Table 5**
Adsorption capacities at different $CO_2$ partial pressures and adsorption efficiency calculated from different materials in the literature.

| Material | mmol N/g | $CO_2$ adsorp(mmol/g) (Pressure) | mmol$CO_2$/mmolN[a] | $CO_2$ adsorp$P$ = 1 atm | Reference |
|---|---|---|---|---|---|
| MCM-48 | 2.28 | 1.09 (0.05 atm) | 0.48 | 1.68 | This work |
| MCM-48 | 2.12 | 1.02 (0.05 atm) | 0.48 | 1.62 | This work |
| MCM-48 | 2.30 | 1.14 (0.05 atm) | 0.49 | 2.05 | [8] |
| MCM-48 | 2.45 | – | – | 0.80 | [11] |
| HMS | 2.28 | – | – | 1.59 | [19] |
| PE-MCM-41 | 4.30 | 2.05 (0.05 atm) | 0.47 | 2.70 | [9] |
| SBA-12 | 2.13 | 0.98 (0.10 atm) | 0.46 | – | [24] |
| SBA-15 | 4.61 | 0.66(0.15 atm) | 0.14 | – | [25] |
| SBA-15 | 2.56 | 0.77(0.05 atm) | 0.30 | – | [26] |

[a] Efficiency reported at the pressure indicated in parentheses.

In view of the above results, the degree of surface functionalization seems to be the main factor in determining the performance of MCM-48 as a $CO_2$ captures material. Fig. 5 represents the $CO_2$ adsorption normalized per unit area as a function of the density of amino groups on the surface. A clear linear correlation can be observed, in agreement with previous literature reports [19]. The only significant deviation is that corresponding to sample functionalized for 5 h, that suffered a structural collapse.

Finally, Table 5 compares the $CO_2$ adsorption capacity for different mesoporous, amino-functionalized silica materials reported in the literature. It could be observed that in general in materials that have some interconnection in between the pores such as the cubic MCM-48, the wormhole like HMS structure [22] and the SBA-12 that shows intergrowth of hexagonal and cubic phases, achieve the highest efficiency. The pore-expanded PE-MCM-41 material, on the other hand, is able to compensate for the lack of a 3-D structure with a high pore volume 2.03 $cm^3/g$, pores of 9 nm, and a highly functionalized surface also giving a $CO_2$/N ratio close to 0.5. In this case it seems likely that larger pore openings in the material would help to prevent possible pore mouth narrowing/plugging due to aminosilane polymerization at the pore openings in the smaller pores of conventional MCM-41 [23]. In the case of the hexagonal SBA-15 lower efficiencies have been encountered.

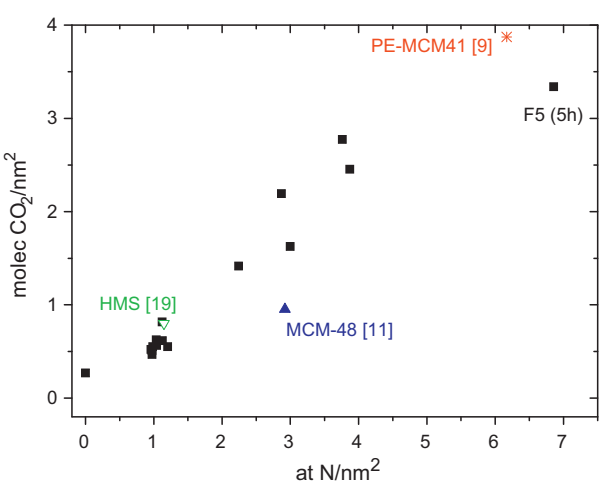


**Fig. 5.** N surface coverage vs. molecules$CO_2/nm^2$ for samples F1 to F15 and literature data.

## 4. Conclusions

A detailed studied of the functionalization conditions for amino-grafted mesoporous MCM-48 material has been carried out. The degree of functionalization in the surface could be tailored varying APTES concentration, time and stirring conditions. There are two requisites to achieve the maximum adsorption efficiency, 0.5 mmol $CO_2$/mol N, under dry conditions and low pressures 5 kPa $CO_2$, which corresponds to chemisorption: (i) total coverage of the surface with the amino groups, to form a surface bidentate carbamate and (ii) to avoid structure collapse after functionalization in order to assure accessibility of the sorbents.

The maximum adsorption capacity achieved at 5 kPa (and therefore corresponding mainly to chemisorbed $CO_2$) was 1.09 mmol $CO_2$/g, which is among the best compared to other materials with similar surface area. There is a correlation between the molecules of $CO_2/nm^2$ and the N atoms/$nm^2$. At higher partial pressures (e.g. around 1 atm of $CO_2$), physical adsorption plays a more substantial role, but even under these conditions for the highest capacity materials prepared in this work, the largest contribution still corresponds to chemisorbed $CO_2$. To maximize the adsorption capacity of the material (chemisorption + physical adsorption), functionalization should maximize the coverage while retaining the ordered structure that maximizes physical adsorption.

## Acknowledgments

Financial support from MICINN, Spain, is gratefully acknowledged. Marta Gil and Inés Tiscornia are grateful to the Government of Aragon (DGA) for financing their grants. We are grateful to Daniel Carmona for carrying out the TEM observations.

## References


[1] S. Choi, J.H. Drese, C.W. Jones, Adsorbent materials for carbon dioxide capture from large anthropogenic point sources, ChemSusChem 2 (2009) 796–854.

[2] F. Su, C. Lu, W. Chen, H. Bai, J.F. Hwang, Capture of $CO_2$ from flue gas via multiwalled carbon nanotubes, Sci. Total Environ. 407 (2009) 3017–3023.

[3] S.C. Hsu, C. Lu, F. Su, W. Zeng, W. Chen, Thermodynamics and regeneration studies of $CO_2$ adsorption on multiwalled carbon nanotubes, Chem. Eng. Sci. 65 (2010) 1354–1361.

[4] S. Couck, J.F.M. Denayer, G.V. Baron, T. Remy, J. Gascón, F. Kapteijn, An amine-functionalized MIL-53 metal-organic framework with large separation power for $CO_2$ and $CH_4$, J. Am. Chem. Soc. 131 (2009) 6326–6327.

[5] Z. Liang, M. Marshall, A.L. Chaffee, $CO_2$ adsorption, selectivity and water tolerance of pillared-layer metal organic frameworks, Microporous Mesoporous Mater. 132 (2010) 305–310.

[6] P.J.E. Harlick, A. Sayari, Applications of pore-expanded mesoporous silica. 5. Triamine grafted material with exceptional $CO_2$ dynamic and equilibrium adsorption performance, Ind. Eng. Chem. Res. 46 (2007) 446–458.

[7] F.-Y. Chang, K.-J. Chao, H.-H. Cheng, C.-S. Tan, Adsorption of $CO_2$ onto amine-grafted mesoporous silicas, Sep. Purif. Technol. 70 (2009) 87–95.

[8] H.Y. Huang, R.T. Yang, D. Chinn, C.L. Munson, Amine-grafted MCM-48 and silica xerogel as superior sorbents for acidic gas removal from natural gas, Ind. Eng. Chem. Res. 42 (2003) 2427–2433.

[9] R. Serna-Guerrero, E. Da'na, A. Sayari, New insights into the interactions of $CO_2$ with amine-functionalized silica, Ind. Eng. Chem. Res. 47 (2008) 9406–9412.

[10] R. Serna-Guerrero, Y. Belmabkhout, A. Sayari, Modeling $CO_2$ adsorption on amine-functionalized mesoporous silica: 1. A semi-empirical equilibrium model, Chem. Eng. J. 161 (2010) 173–181.

[11] S. Kim, J. Ida, V.V. Guliants, J.Y.S. Lin, Tailoring pore properties of MCM-48 silica for selective adsorption of $CO_2$, J. Phys. Chem. B 109 (2005) 6287–6293.

[12] B. Margandan, J.Y. Lee, A. Ramani, H.T. Jang, Synthesis of chloropropylamine grafted mesoporous MCM-41, MCM-48 and SBA-15 from rice husk ash: their application $CO_2$ chemisorption, J. Porous Mater. 17 (2010) 475–484.

[13] J.M. Kim, S.K. Kim, R. Ryoo, Synthesis of MCM-48 single crystals, Chem. Commun. 2 (1998) 259–260.

[14] H. Ritter, M. Nieminen, M. Karppinen, D. Brühwiler, A comparative study of the functionalization of mesoporous silica MCM-41 by deposition of 3-aminopropyltrimethoxysilane from toluene and from the vapor phase, Microporous Mesoporous Mater. 121 (2009) 79–83.

[15] H. Ritter, D. Brühwiler, Accessibility of amino groups in postsynthetically modified mesoporous silica, J. Phys. Chem. C 113 (2009) 10667–10674.

[16] C.T. Kresge, M.E. Leonowicz, W.J. Roth, J.C. Vartulli, J.S. Beck, Ordered mesoporous molecular sieves synthesized by a liquid-crystal template mechanism, Nature 359 (1992) 710–712.

[17] L.T. Zhuravlev, Concentration of hydroxyl groups on the surface of amorphous silicas, Langmuir 3 (1987) 316–318.

[18] D. Kumar, K. Schumacher, C. du Fresne von Hohenesche, M. Grün, K.K. Unger, MCM-41, MCM-48 and related mesoporous adsorbents: their synthesis and characterization, Colloids Surf. A: Physicochem. Eng. Aspects 187–188 (2001) 109–116.

[19] G.P. Knowles, J.V. Graham, S.W. Delaney, A.L. Chaffee, Aminopropyl-functionalized mesoporous silicas as $CO_2$ adsorbents, Fuel Process. Technol. 86 (2005) 1435–1448.

[20] A. Nieto, F. Balas, M. Colilla, M. Manzano, M. Vallet-Regí, Functionalization degree of SBA-15 as key factor to modulate sodium alendronate dosage, Microporous Mesoporous Mater. 116 (2008) 4–13.

[21] T. Linssen, K. Cassiers, P. Cool, E.F. Vansant, Mesoporous templated silicates: an overview of their synthesis, catalytic activation and evaluation of the stability, Adv. Colloid Interface Sci. 103 (2003) 121–147.

[22] W. Zhang, T.R. Pauly, T.J. Pinnavaia, Tailoring the framework and textural mesopores of HMS molecular sieves through an electrically neutral ($S^{\circ}I^{\circ}$) assembly pathway, Chem. Mater. 9 (1997) 2491–2498.

[23] P.J.E. Harlick, A. Sayari, Applications of pore-expanded mesoporous silicas. 3. Triamine silane grafting for enhanced $CO_2$ adsorption, Ind. Eng. Chem. Res. 45 (2006) 3248–3255.

[24] V. Zelenak, D. Halamova, L. Gaberova, E. Bloch, P. Llewellyn, Amine-modified SBA-12 mesoporous silica for carbon dioxide capture: effect of amine basicity on sorption properties, Microporous Mesoporous Mater. 116 (2008) 358–364.

[25] N. Hiyoshi, K. Yogo, T. Yashima, Adsorption characteristics of carbon dioxide on organically functionalized SBA-15, Microporous Mesoporous Mater. 84 (2005) 357–365.

[26] L. Wang, L. Ma, A. Wang, Q. Liu, T. Zhang, $CO_2$ adsorption on SBA-15 modified by aminosilane, Chin. J. Catal. 28 (9) (2007) 805–810.